PROTEINS: Structure, Function, and Genetics 13:87–99 (1992)

Mutating the Charged Residues in the Binding Pocket of Cellular Retinoic Acid-Binding Protein Simultaneously Reduces Its Binding Affinity to Retinoic Acid and Increases Its Thermostability

Jianhua Zhang,[1] Zhi-Ping Liu,[2] T. Alwyn Jones,[3] Lila M. Gierasch,[1,2] and Joseph F. Sambrook[1]
Departments of [1]Biochemistry and [2]Pharmacology, University of Texas Southwestern Medical Center at Dallas, Dallas, Texas, 75235 and [3]Department of Molecular Biology, Biomedical Center, S-751 24 Uppsala, Sweden

ABSTRACT **Three-dimensional modeling of the complex between retinoic acid-binding protein (CRABP) and retinoic acid suggests that binding of the ligand is mediated by interaction between the carboxyl group of retinoic acid and two charged amino acids (Arg-111 and Arg-131) whose side chains project into the barrel of the protein. To assess the contribution of these amino acids to protein–ligand interaction, amino acid substitutions were made by oligonucleotide-directed, site-specific mutagenesis. The wild-type and mutant proteins were expressed in *E. coli* and subsequently purified. Like wild-type CRABP, the mutant proteins are composed mainly of β-strands as determined by circular dichroism in the presence and absence of ligand, and thus presumably are folded into the same compact barrel structure as the wild-type protein. Mutants in which Arg-111 and Arg-131 are replaced by glutamine bind retinoic acid with significantly lower affinity than the wild-type protein, arguing that these two residues indeed interact with the ligand. The mutant proteins are more resistant to thermal denaturation than wild-type CRABP in the absence of retinoic acid, but they are not as thermostable as the CRABP–retinoic acid complex. These data suggest a model for CRABP–retinoic acid interaction in which the repulsive forces between the positively-charged arginine residues provide conformational flexibility to the native protein for retinoic acid to enter the binding pocket. Elimination of the positively-charged pair of amino acids produces a protein that is more thermostable than wild-type CRABP but less effective at ligand-binding.**

Key words: β-barrel, protein engineering, protein folding, electrostatic interactions, protein–ligand interaction

INTRODUCTION

Cellular retinoic acid-binding protein (CRABP) is a member of a family of intracellular β-barrel proteins that bind hydrophobic ligands.[1,2] Its particular ligand, retinoic acid, has dramatic effects on morphogenesis of vertebrate embryos and induces differentiation of cultured cells.[3,4] CRABP is present in a variety of cells and tissues and is expressed at different levels in different parts of developing embryos.[5] However, CRABP is not believed to be directly involved in the tissue-specific activation of genes that accompanies differentiation. Instead, activation of retinoic acid-responsive genes is believed to involve nuclear proteins that belong to the family of steroid receptors and are themselves expressed in a tissue-specific fashion.[6,7] The binding of retinoic acid (RA) to these receptors, and their subsequent interaction with *cis*-acting control elements, may regulate the transcription of target genes in the cells. If CRABP has a role in these processes, it can be only subsidiary—perhaps in transporting RA through the cell or in regulating the concentration of retinoic acid.[8,9]

In addition to CRABP, the family of related β-barrel proteins includes cellular retinol-binding proteins (CRBP and CRBPII), rat fatty acid-binding proteins (intestinal fatty acid-binding protein, I-FABP, liver fatty acid-binding protein, L-FABP, heart fatty acid-binding protein, H-FABP), murine adipocyte P2 protein, and bovine myelin P2 protein. These protein typically contain identical or similar amino acids at homologous positions and, in every case, are encoded by genes that contain four exons and three introns.[10] The three-dimensional structures of two of these proteins, myelin P2 protein and I-FABP, have been determined by X-ray crystal-

Received April 18, 1991; revision accepted June 11, 1991.
Address reprint requests to Joseph F. Sambrook, Department of Biochemistry, Univ. of Texas Southwestern Medical School, 5323 Harry Hines Blvd., Dallas, TX 75235-9038.

Abbreviations: 2ME, 2-mercaptoethanol; CD, circular dichroism; CRBP, cellular retinol-binding protein; CRBPII, cellular retinol-binding protein II; CRABP, cellular retinoic acid-binding protein; EDTA; ethylenediaminetetraacetic acid; I-FABP, intestinal fatty acid-binding protein; PMSF, phenylmethylsulfonyl fluoride; RA, retinoic acid; SCRs, structurally conserved regions; SDS, sodium dodecyl sulfate.

TABLE I. Sequence Alignment of CRABP With Myelin P2 Protein and I-FABP*

```
                  | **************   SCR1   ****************************************
CRABP#            1                 11                  21                  31
CRABP             P-N-F-A-G-T-W-K-M-R-S-S-E-N-F-D-E-L-L-K-A-L-G-V-N-A-M-L-R-K-V-A-V-A-
myelinP2#       1                   11                  21                  31
myelinP2        S-N-K-F-L-G-T-W-L-L-V-S-S-E-N-F-D-E-Y-M-K-A-L-G-V-G-L-A-T-R-K-L-G-N-L-
I-FABP            M-A-F-D-G-T-W-K-V-Y-R-N-E-N-Y-E-K-F-M-E-K-M-G-I-N-V-V-K-R-K-L-G-A-H-

                 *|     | ******************   SCR2   ********************************
CRABP#                     41                  51                  61
CRABP             A-A-S-K-P-H-V-E-I-R-Q-D-G-D-Q-F-Y-I-K-T-S-T-T-V-R-T-T-E-I-N-F-K-V-G-
myelinP2#                41                  51                  61
myelinP2          A------K-P-R-V-I-I-S-K-K-G-D-I-I-T-I-R-T-E-S-P-F-K-N-T-E-I-S-F-K-L-G-
I-FABP            D------N-L-K-L-T-I-T-Q-E-G-N-K-F-T-V-K-E-S-S-N-F-R-N-I-D-V-V-F-E-L-G-

                  ************************************|     |*****   SCR3   ****|
CRABP#               71                  81                  91                 101
CRABP             E-G-F-E-E-E-T-V-D-G-R-K-C-R-S-L-P-T-W-E-N-E-N-K-I-H-C-T-Q-T-L-L-E-G-
myelinP2#            71                  81                  91
myelinP2          Q-E-F-E-E-T-T-A-D-N-R-K-T-K-S-T-V-T-L-A-R---G-S-L-N-Q-V-Q-K-W-N-----
I-FABP            V-D-F-A-Y-S-L-A-D-G-T-E-L-T-G-T-L-T-M-E-G---N-K-L-V-G-K-F-K-R-V-D-N-

                    |************************   SCR4   ****************************|
CRABP#                        111                 121                 131
CRABP             D-G-P-K-T-Y-W-T-R-E-L-A-N-D-E-L-I-L-T-F-G-A-D-D-V-V-C-T-R-I-Y-V-R-E-
myelinP2#            101                 111                 121                 131
myelinP2          --G-N-E-T-T-I-K-R-K-L-V-D-G-K-M-V-V-E-C-K-M-K-D-V-V-C-T-R-I-Y-E-K-V-
I-FABP            --G-K-E-L-I-A-V-R-E-I-S-G-N-E-L-I-Q-T-Y-T-Y-E-G-V-E-A-K-R-I-F-K-K-E-
```

*The sequences of CRABP, myelin P2 protein, I-FABP are aligned in this table. The structurally conserved regions (SCRs) are marked as |***SCR***|. The amino acid number in CRABP sequence is labeled on top of the CRABP sequence. The amino acid numbers in myelin P2 protein and I-FABP are labeled on top of the myelin P2 sequence. The Arg-111, Arg-131, and Tyr-133 residues that are conserved between CRABP, myelin P2, and I-FABP proteins are shown in shadows. They are replaced by Gln, Gln, and Phe in CRBP II.

lography.[10–12] Both proteins are compact, 10-stranded, up-and-down β-barrels that encapsulate the fatty acid ligand. Although only 28.7% of their amino acid residues are identical, the two proteins display three-dimensional structures that are virtually superimposable (rms difference <1.8 Å). It has been suggested that ligand specificity in this family of proteins is determined by the nature and distribution of the amino acid side chains pointing into the cavity of the β-barrel to make contact with the ligand molecule.[10]

In the crystal structure of the complex of I-FABP and palmitate, the negatively charged carboxylate group of the fatty acid forms a five-membered hydrogen bonding network with Arg-106, Gln-115 (which have been aligned to Arg-111 and Leu-120 in CRABP,[10] Table I), and two ordered solvent molecules.[12] In the network, two hydrogen bonds are formed between the fatty acid carboxylate and the guanidinium group of Arg-106. Other hydrogen bonds in this network include one between the side chain oxygen of Gln-115 and the NH^{ϵ} of Arg-106, and three in series between the NH_2 of Gln-115, two water molecules and fatty acid. In the three-dimensional structure of fatty acid bound-bovine myelin P2 protein determined at 2.7 Å resolution, Arg-106 and Arg-126 (which have been aligned to Arg-111 and Arg-131 in CRABP,[10] Table I) are buried in the β-barrel. The initial study showed the carboxyl group of the ligand to be located between the guanido group of the two arginines and close to the hydroxyl group of Tyr-128 (Tyr-133 in CRABP,[10] Table I). Subsequent crystallographic refinement shows hydrogen bonds from the carboxylate to both Arg-106 and Tyr-128, while Arg-126 is in proximity but not involved in hydrogen bond formation (Cowan, Newcomer and Jones, in preparation). In β-barrel proteins whose ligands do not carry carboxylate groups (for example, CRBP and CRBPII, which specifically bind all-*trans*-retinol and/or all *trans*-retinal), the positions corresponding to the two arginine residues and the tyrosine are occupied by Gln, Gln, and Phe.[10] However, as in myelin P2 protein, the two arginines and the tyrosine are conserved in CRABP. These arginine residues of CRABP may form electrostatic bonds with the carboxyl group of retinoic acid.

This paper describes the ligand-binding properties and thermal stabilities of a set of mutants of CRABP in which either or both Arg-111 and Arg-131 have been changed to Gln-111 and Gln-131. The mutant proteins retain largely wild-type conformations. We find that one of the two Arg residues (Arg-111) is more critical to ligand binding, although both argin-

ines contribute significantly. Interestingly, the mutants lacking one or both of the arginines are more thermostable than the wild-type protein.

MATERIALS AND METHODS

Materials

All-*trans*-retinoic acid, all-*trans*-retinol, all-*trans*-retinal, and *N*-acetyl-L-tryptophanamide were purchased from Sigma (St. Louis, MO). A full-length cDNA encoding murine CRABP was cloned from a library synthesized from poly(A^+) RNA extracted from 12-day mouse embryos and established in the bacteriophage λ vector gt10 library. This library was kindly provided by Dr. Gail Martin, UCSF. The library was screened with a full-length bovine CRABP cDNA probe[13,14] at high stringency (hybridized at 67°C for 16 hr; washed sequentially at room temperature with 6 × SSC, at 67°C with 2 × SSC, and 0.1% SDS for 30 min, and at 67°C with 0.2 × SSC and 0.1% SDS for 30 min). From 100,000 plaques, 24 positives were obtained from the initial screen. After secondary screening, 16 positives were isolated from the original 24. Candidate clones were subsequently put into plasmid pUC119, which carries the origin of DNA replication and packaging signal of the single-stranded bacteriophage M13.[15] The resulting recombinant plasmid was used to transform *E. coli* XL1-blue, which carries an F′ episome. Single-stranded DNA was harvested from progeny bacteriophage produced after infection of the transformed cells with a helper virus M13K07[15] and sequenced from both ends. Universal primer was used for initial sequencing and successive synthetic oligos were then synthesized at 300 bp intervals and used to obtain the complete sequences. Two clones [752 bp and 1.1 kb plus poly(A) tail] contained sequences coding for the entire CRABP protein. These two clones have identical sequences except that the 1.1 kb clone has longer untranslated 5′ and 3′ sequences. The coding region has 90% sequence homology with bovine CRABP at the nucleotide level and encodes a protein whose amino acid sequence is identical to bovine CRABP.

Modeling of CRABP

An atomic model of retinoic acid-bound CRABP was constructed using the refined crystal structure of bovine myelin P2 protein as a template and a primary structure alignment[10] shown in Table I. Modeling was performed in four major steps using the program "Homology"[16] on a Silicon Graphics Personal Iris computer. The first step was to identify the structurally conserved regions (SCRs) and nonconserved regions such as insertions and deletions (also called loop regions in the Homology program). Second, after the correspondence between the P2 and CRABP sequences had been optimized, the coordinates for the SCRs were transferred from myelin P2 protein to CRABP. Whenever identical amino acids were present in corresponding positions in both proteins, all of the relevant coordinates were transferred. When different amino acids were present at corresponding positions, only the coordinates for the main polypeptide chain were transferred, while side chain atoms were adjusted automatically to reflect the residue present in CRABP. Third, the loop regions were built using the loopsearch option of the Homology program. This option searches a structural database for fragments from proteins of known structure. The fragments are selected to have the same number of amino acids as a given loop region in the CRABP model, and residues at starting and ending positions with properties similar to those required by the loop to be modeled.[17] Lastly, the monoclinic crystal structure of retinoic acid[18] was superimposed onto the ligand position of myelin P2 protein, and the model was refined by energy minimization using the program Discover[16] with maximum coordinate derivatives less than 0.05 kcal/Å. The parameters for the force field used are described elsewhere.[19]

The model structure of the retinoic acid–CRABP complex after energy minimization was then used to construct a model of CRABP by removing retinoic acid from the complex. The model structure of the double mutant form of CRABP (R111Q,R131Q) was obtained by replacing R111 and R131 with glutamines in the CRABP model. Both model structures were again energy minimized.

Calculation of Electrostatic Potentials of CRABP-RA Complex, CRABP, and the Double Mutant Version of CRABP (R111Q,R131Q)

The calculation of electrostatic potentials was carried out using the Poisson–Boltzmann method,[20,21] assuming a dielectric constant of 2 for the interior of the proteins and 80 for the exterior, and an ionic strength in the aqueous solution of 0.145 M. The interior and exterior of the protein were defined by the solvent accessible surface area including the cavity in the binding pocket. The following scheme was used to assign charges to the atomic coordinates of charged residues: the ε nitrogen of each lysine, +1; N-terminal proline residue, +1; each guanidinium nitrogen, +0.5; two aromatic nitrogens of histidines, +0.25 each; each carboxylate oxygen, −0.5; and C-terminal carboxyl of glutamate, −1. The calculation was performed on the Silicon Graphics Personal Iris computer using the program Delphi.[16]

Oligonucleotide-Directed Mutagenesis

Site-directed mutagenesis was performed by the method of Zoller and Smith[22] as described.[15] Single-stranded DNA was generated from plasmid pUC119 containing full-length murine CRABP cDNA and used as a template to create mutant CRABP–R111Q and CRABP–R131Q. The oligonucleotides used, and the mutations generated are summarized in Table

TABLE II. Mutagenesis of CRABP

Name of mutant*	Mutation(s)	Name of template DNA use for mutagenesis sequence of mutagenic oligonucleotide (5'-3')
R111Q	Arg-111 → Q	Mutation of CRABP with oligonucleotide Q1 CCAGCTCTTGGGTCCAG
R131Q	Arg-131 → Q	Mutation of CRABP with oligonucleotide Q2 CATAAATTTGTGTGCACAC
R111Q,R131Q	Arg-111 → Q Arg-131 → Q	Mutation of R111Q with oligonucleotide Q2

*Those mutants have then been further mutated to introduce the *Nde*I site upstream of initiating ATG with oligonucleotide NGTTGGGCATATGGGCAGTG

II. CRABP–R111Q,R131Q was generated from CRABP–R111Q by a second round of mutagenesis during oligonucleotide Q2 (Table II). cDNAs encoding wild-type CRABP, the two point mutants R111Q and R131Q, and the double mutant R111Q,R131Q were then further modified by site-directed mutagenesis to introduce an *Nde*I site at the initiating ATG codon. The entire sequence of wild-type CRABP and sequences of all mutants were then verified by DNA sequencing.

Expression and Purification of the Proteins

The coding regions of cDNAs encoding wild-type and mutant versions of CRABP were recovered by digestion with restriction endonucleases *Nde*I and *Eco*RI and subcloned into the *E. coli* expression vector pT7-7 (generously provided by Dr. S. Tabor, Harvard University, ref. 23). In the resulting plasmids, the sequences encoding CRABP are placed downstream of the bacteriophage T7 promoter and a strong *E. coli* ribosome-binding site. Subcloning into *Nde*I site ensures that the cDNA is in frame with the initiating ATG codon in the expression vector. A similar recombinant plasmid was constructed using the cDNA sequence encoding cellular retinol-binding protein (CRBPII, a kind gift from Dr. J. Gordon, Washington University, St. Louis). Strains of *E. coli* were established carrying each of these recombinant plasmids and plasmid pGP1-2 (also a gift from Dr. S. Tabor, ref. 23). Plasmid pGP1-2 contains the gene encoding bacteriophage T7 RNA polymerase gene under the control of the inducible bacteriophage λP_L promoter and the gene for the temperature-sensitive repressor, cI857. Synthesis of wild-type and mutant versions of CRABP and of CRBPII was induced after raising the temperature briefly to 42°C.[14,22] These proteins were then purified as described below using a modification of the procedure previously used to purify CRBPII.[24]

For large-scale purification, freshly transformed *E. coli* DH-1 carrying pT7-7-CRABP and pGP1-2 was grown overnight at 30°C in LB broth containing 20 μg/ml carbenicillin and 20 μg/ml kanamycin. The cultures were then diluted to 500 ml TB (2% tryptone, 1% yeast extract, 0.5% NaCl, 0.2% glycerol, 50 mM KPO_4 pH 7.2, 20 μg/ml carbenicillin, and 20 μg/ml kanamycin) and incubated for a further 16 hr at 30°C. Late log-phase cultures were inoculated into 10 liters of TB and incubated in an automatic fermenter for a further 8 hr at 37°C. The temperature of the cultures was then raised to 42°C for 30 min, followed by incubation for 12 hr at 37°C. Cells were harvested by centrifugation at 4°C, suspended in 10% glycerol, and frozen in liquid nitrogen. The frozen cell paste (40 g) was resuspended in 100 ml homogenization buffer (2 mM PMSF, 10 mM Tris-Cl pH 7.6, 1 mM EDTA, 1 mM 2ME, 10% sucrose, 0.05% sodium azide), and lysed by blending in a bead beater for 6 min on ice. After centrifugation at 41,000*g* for 20 min, CRABP was detected in the supernatant as a prominent band after electrophoresis and Coomassie staining in a 15% polyacrylamide-SDS gel. The subsequent four-step purification procedure involved (1) precipitation with 50–70% ammonium sulfate, (2) chromatography through G-50 Sephadex (5 cm × 1.5 m) in 10 mM KPO_4 (pH 8.0), 2 mM PMSF, 1 mM 2ME, 1 mM EDTA, 0.05% sodium azide, 200 mM NaCl, (3) ion-exchange chromatography on DEAE-trisacryl (2.6 × 7.6 cm) equilibrated in 10 mM Tris-Cl (pH 8.3), 2 mM PMSF, 0.05% sodium azide, and eluted with 0–0.2 M NaCl gradient in a total volume of 500 ml, and (4) ion-exchange chromatography on DEAE-trisacryl column (2.6 × 3.8 cm) equilibrated in 0.01 M imidazole acetate (pH 6.0), 2 mM PMSF, 0.05% sodium azide, and eluted with 0.01–0.1 M imidazole acetate gradient in a total volume of 500 ml. Fractions containing CRABP that was assessed to be >90% pure by SDS polyacrylamide gel electrophoresis were combined and dialyzed against 10 mM Tris-Cl (pH 8.3), 1 mM 2ME, 1 mM EDTA, 0.05% sodium azide and stored at 4°C.

Fluorimetric Titration

Steady-state fluorescence was measured with a photon counting spectrofluorimeter (model Greg PC, ISS Inc.). Solutions of wild-type and mutant versions of CRABP were prepared at concentrations ranging from 0.5 to 3 μM in 10 mM sodium phosphate pH 7.0, 150 mM NaCl. Working solutions of

retinoic acid were prepared in absolute ethanol, and their concentrations were determined spectrophotometrically using a molar absorption coefficient of 45,000 M^{-1} cm^{-1} at 336 nm.[25]

Binding of retinoic acid was measured by a fluorimetric titration method.[25] Wild-type and mutant CRABP proteins were excited at 280 nm (1 nm slit width), while CRBPII was excited at 296 nm. The emission spectra from 300 to 370 nm were recorded at 1 nm slit width for each increasing concentration of retinoic acid. *N*-Acetyltryptophanamide was used as a blank. Retinoic acid was added in 2-μl aliquots with the final added volume not exceeding 1% of the protein solution. The apparent dissociation constant of a single binding site (K_d) and the number of binding sites (n) for retinoic acid binding to CRABP were evaluated by linear least squares plots of Eq. (1).

$$P_0\alpha = \frac{R_0}{n} \times \frac{\alpha}{(1-\alpha)} - \frac{K_d}{n} \quad (1)$$

where α is the fraction of free binding sites, R_0 is the retinoic acid concentration at each point, P_0 is the protein concentration, and K_d is the calculated dissociation constant. The value of α was calculated for every point on the titration curve of fluorescence intensity vs. retinoic acid concentration using Eq. (2),

$$\alpha = \frac{(F-F_{max})}{(F_0-F_{max})} \quad (2)$$

where F is the intensity of fluorescence at 324 nm (the wavelength of maximum emission of fluorescence) at a certain concentration of retinoic acid, F_{max} represents the intensity of fluorescence after saturation of all the apoprotein with the ligand, and F_0 is the initial intensity of fluorescence.

Circular Dichroism (CD)

CD spectra were recorded on an Aviv model 60DS instrument. The concentrations of the protein solutions were determined by quantitative amino acid analysis. To record CD spectra from 190 to 250 nm, protein solutions were prepared at a concentration of 3 μM in 10 mM potassium phosphate buffer (pH 7.0) and measurements were taken using a 2 mm pathlength cell. To record CD spectra for the complexes of retinoic acid–CRABP and retinoic acid–CRABP mutants in the range from 300 to 450 nm, protein solutions were prepared at a concentration of 20 μM in 10 mM Tris-Cl (pH 8.3), and measurements were taken using a 5 mm pathlength cell.

Mean residue ellipticity, $[\theta]_M$ (in millidegrees), is calculated from the measured θ using Eq. (3),

$$[\Theta]_M = \frac{\Theta \times 100}{(C \times d \times N)} \quad (3)$$

where θ is the measured ellipticity in millidegrees, C is the molar protein concentration, d is the pathlength in cm, and N is the number of peptide bonds in the protein.

To follow the thermal denaturation of wild-type and mutant versions of CRABP, CD spectra were monitored at a single wavelength (205 nm) where the differences of CD signals between folded and unfolded states of the protein are most significant. The temperature of the protein solution was raised at a rate of 1°C every 2 min through the range 25–80°C. In the case of wild-type CRABP, a heating rate of 1°C per 10 min was also used to ensure that the system had sufficient time to reach equilibrium. No differences were observed between the curves obtained with different heating rate.

The equilibrium constant (K) between the folded and unfolded conformers of the protein, and the free energy, ΔG, can be calculated using Eqs. (4) and (5) for each temperature,

$$K = \frac{f_u}{(1-f_u)} \quad (4)$$

$$\Delta G = -RT \ln K \quad (5)$$

where f_u is the fraction of unfolded protein, R is the gas constant (1.987 cal/deg/mol), and T is the absolute temperature.

We have plotted ΔG as a function of temperature (data not shown). At the melting temperature, T_m,

$$\Delta G(T_m) = 0 = \Delta H_m - T_m \times \Delta S_m. \quad (6)$$

The entropy change at the melting temperature, ΔS_m, can be calculated from the slope of the curve at T_m. The enthalpy change at the melting temperature, ΔH_m, can be calculated from $T_m \times \Delta S_m$. To determine the differences in conformational stability among proteins that vary slightly in structure (e.g., as a consequence of the structural changes achieved by site-directed mutagenesis or chemical modification), $\Delta(\Delta G)$ were calculated by Eq. (7).[26,27]

$$\Delta(\Delta G) = [\Delta(T_m)] \times \Delta S_m \quad (7)$$

where $\Delta(T_m)$ is the difference in melting temperature between mutant versions of the protein, or the ligand-bound form of the protein and the wild-type protein, ΔS_m is the value for the wild-type protein at the melting temperature. This equation is valid only in cases where the enthalpy change is negligible over the temperature range compared.

RESULTS

Modeling the Structure of CRABP

The family of intracellular proteins that bind hydrophobic ligands is believed to share a similar tertiary structure.[1,2,10–12] The crystal structures of two members of this family, I-FABP and myelin P2 protein, have been refined to 1.7 and 2.7 Å, respectively.[10–12] Although only 28% of their amino acid residues are identical, the two proteins display

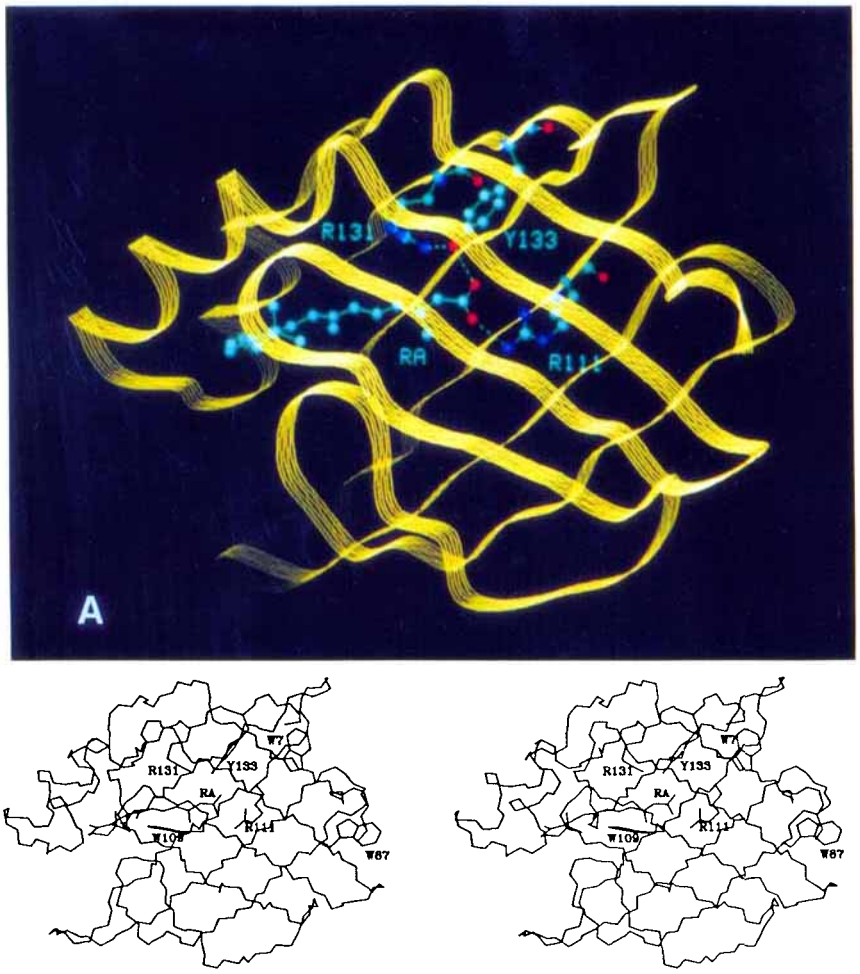

Fig. 1. Model structure of CRABP. (**A**) Ribbon representation of CRABP. Also shown are retinoic acid, residues Arg-111, Arg-131, and Tyr-133. (**B**) Stereo C_α chain drawing of CRABP with bound retinoic acid. Also shown are Arg-111, Arg-131, Tyr-133, and Trp residues (Trp-7, Trp-87, and Trp-109). The hydrogen bonds between the carboxyl group of the retinoic acid and the Arg-111, Arg-131, and Tyr-133 are shown in dotted lines.

three-dimensional structures that are virtually superimposable (rms difference <1.8 Å for C_α positions). Both proteins consist of two nearly orthogonal β-sheets formed by 10 antiparallel β-strands.

A comparison of the amino acid sequences of murine CRABP, I-FABP, and myelin P2 protein is shown in Table I. The sequence alignment described by Jones et al.[10] was used to determine the structurally conserved regions (SCRs). Three insertions were found in the sequence alignment: A36-S37, E90, and E101-G102-D103. These are all in loop regions in myelin P2 protein, as would be expected since loop regions can tolerate more variations. Atomic coordinates of CRABP SCRs were obtained from the corresponding residues of the P2 protein. Those of the insertion regions were obtained from the Brookhaven Data Bank by using the loopsearch option of the Homology program (see Materials and Methods). No major steric clashes resulted at this step of the modeling. Side chain contacts were removed by subsequent energy minimization refinement. Two different energy minimizations were carried out; in one case, all the side chains were kept neutral; in the other, charge of +1 were assigned for Arg/Lys side chains and charge of −1 were assigned for Asp/Glu side chains. In both energy minimizations, the carboxyl group of the ligand retinoic acid was assigned charge −1. The resulting structures are similar and the binding modes of retinoic acid to CRABP are identical. The overall structure of CRABP is superimposable with myelin P2 protein. The rms difference between the positions of the C_α atoms of myelin P2 protein and the modeled structure of CRABP is 1.7 Å. The interior residue positions of myelin P2 protein are conserved in the model structures of CRABP (with and without bound retinoic acid). Figure 1A shows a ribbon representation of the modeled structure of CRABP with

the orthogonal β-sheets and the predicted location of retinoic acid inside the barrel. Side chains of Arg-111, Arg-131, Tyr-133 are also shown. They are in proximity to the carboxyl end of retinoic acid. Figure 1B shows the α-carbon drawing of CRABP with the retinoic acid, the three tryptophans, and Arg-111, Arg-131, and Tyr-133 residues in close contact with retinoic acid. The carboxyl group of retinoic acid is located between Arg-111 and Arg-131 before energy minimization. After energy minization, the hydrocarbon chain of retinoic acid is bent so that its carboxyl group forms two hydrogen bonds with Arg-111. In this modeled binding arrangement, Arg-131 is not directly involved in the interaction with retinoic acid. Instead, the guanidinium group of its side chain forms hydrogen bonds with Tyr-133, –OH, the hydroxyl proton of which also forms another hydrogen bond with the carboxyl group of retinoic acid. It is important to note that no water molecules are included in the calculation. This could affect the hydrogen bonding network described above. Nevertheless the modeled structure of the RA–CRABP complex provides a working hypothesis for testing the role of interior arginine residues in ligand binding. Arg-111 and Arg-131 are conserved in β-barrel proteins that bind carboxylic acids (I-FABP and myelin P2 protein), but are replaced by Gln and Gln, respectively, in proteins that bind the alcohol form of retinoid (CRBP and CRBPII).[10] Thus, modeling of CRABP against the known structure of the myelin P2 protein indicates that the specificity and affinity of CRABP for its ligand may be determined by electrostatic interactions formed between the basic side chains of Arg-111 and Arg-131 and the negatively charged carboxyl group of retinoic acid.

Electrostatic Potential of Wild-Type CRABP With and Without Ligand, and of the Double Mutant R111Q,R131Q

At neutral pH, CRABP is negatively charged (net charge of −3), which might be expected to lead to general repulsion of the retinoic acid ligand. To characterize further the interaction between CRABP and retinoic acid, we calculated the electrostatic potentials of wild-type CRABP with and without bound retinoic acid, and of the double mutant R111Q,R131Q using the modeled structure of CRABP described in the previous section. Figure 2 shows a section through the electrostatic potential surfaces calculated with wild-type CRABP, the double mutant R111Q,R131Q, and wild-type CRABP with the retinoic acid ligand bound (CRABP + RA). Not surprisingly, the potential fields inside the putative binding pocket are drastically different in all three cases. There is a well-defined positive potential field inside the wild-type CRABP which extends out into the solvent (shown in light and dark blue). This large positive potential field inside the binding pocket is no longer seen in the double mutant R111Q,R131Q. The positive potential field seen inside wild-type CRABP could provide a target area for the negatively charged retinoic acid, thus enhancing the binding. At the same time, it could provide a potential field to guide the entrance of retinoic acid into the binding pocket. Substituting Arg-111 and Arg-131 with Glns would be expected to abolish such favorable interactions between CRABP and retinoic acid.

Site-Directed Mutagenesis of the CRABP Protein

To test the hypothesis that ligand binding in CRABP is mediated by the electrostatic interaction between the arginine residues of CRABP and the retinoic acid, mutations were created by the oligonucleotide-mediated, site-directed mutagenesis of murine CRABP cDNA. The single mutants R111Q, R131Q, and the double mutant R111Q,R131Q altered the putative ligand-binding site of CRABP in a way that was predicted to affect the electrostatic interactions between the CRABP protein and retinoic acid. Wild-type and mutant versions of CRABP were expressed in *E. coli* and purified as described in Materials and Methods. The identities and purities of the proteins were assessed by polyacrylamide SDS-gel electrophoresis with Coomassie-blue staining, HPLC chromatography, N-terminal sequencing after Edman degradation, and amino acid composition analysis. The proteins are 95% pure.

Structural Comparison of Wild-Type and Mutant Versions of CRABP

To verify that the mutant proteins have properly folded, we measured the CD spectra of the wild-type and the mutant proteins in the conformationally diagnostic far-UV wavelength range between 190 and 250 nm. All the mutant forms of CRABP showed a CD spectrum similar to that of wild-type CRABP with a minimum CD band at 216 nm (Fig. 3). Studies of model polypeptides and proteins[28–31] have shown that a CD minimum at this wavelength arises from a highly ordered β-structure. These observations from CD spectra suggest that the overall structures of the mutant versions of CRABP are similar to that of wild-type CRABP, although local differences in structures of these proteins also exist. The most obvious difference is at wavelength 230 nm region. Although a shoulder could be observed with wild-type CRABP and one of the single mutants of CRABP (R131Q), it is not as distinct in R111Q, or in the double mutant R111Q,R131Q (see discussion). As expected, CRBPII also shows a predominantly β structure with more intensity at 216 nm and no second peak at 230 nm. This may be due to small structural differences between these two proteins, or, alternatively, it may reflect a more rigid overall structure of CRBPII compared to CRABP.

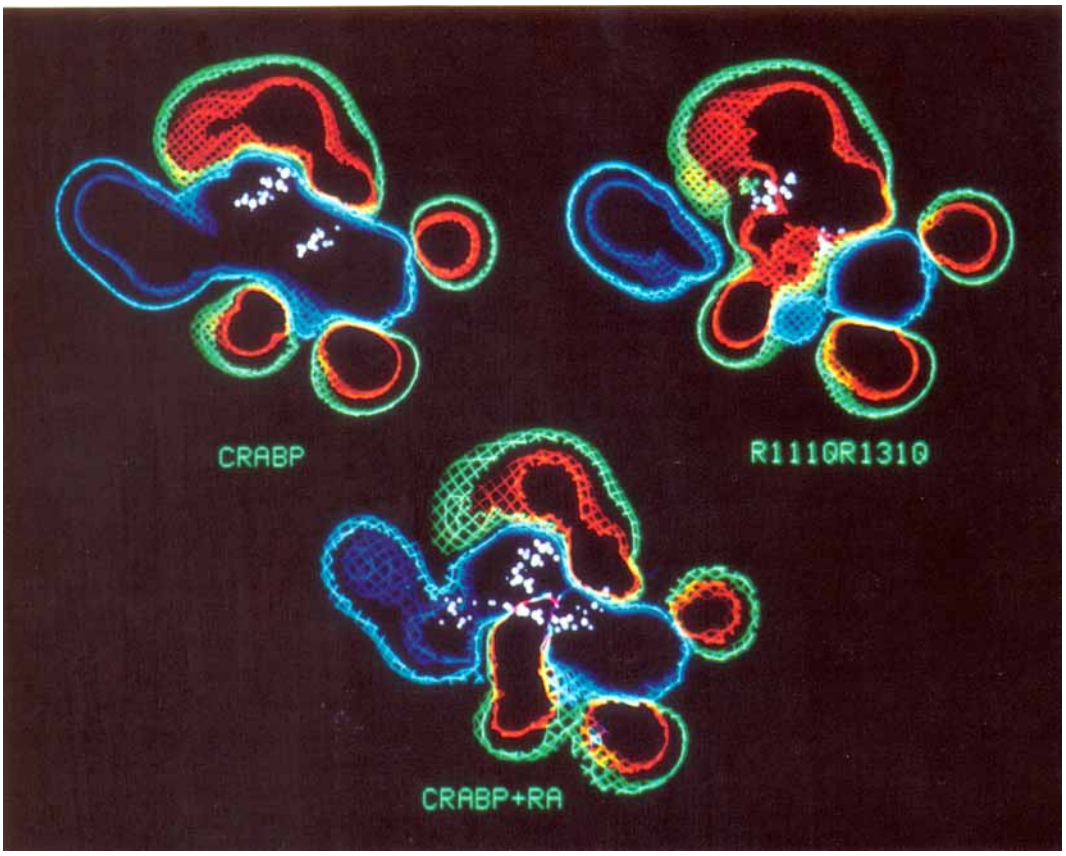

Fig. 2. Slices through the electrostatic potentials of wild-type CRABP, double mutant R111Q,R131Q, and wild-type CRABP with bound retinoic acid. The slices are taken in the plane of the residues R111, R131, and retinoic acid. The contours are shown at levels of 0.5 kT (light blue), 1 kT (dark blue), −0.5 kT (green), and −1 kT (red). The coordinates of the proteins are from computer modeling (see Materials and Methods). The electrostatic potential fields are calculated using the Poisson–Boltzmann method. The potentials around the surfaces of the three proteins are similar. However, the positive potential extended to the solvent from the binding pocket of wild-type CRABP is no longer seen in double mutant and is weaker in wild-type CRABP with bound retinoic acid.

Ligand-Binding Properties of Wild-Type and Mutant CRABP Proteins

Fluorimetric titrations were used to measure the binding affinities of wild-type and mutant versions of CRABP for retinoic acid.[25] When CRABP is complexed with retinoic acid, its intrinsic fluorescence is quenched by 70% (Fig. 4a) in our experimental conditions. By monitoring the progressive quenching of the CRABP emission spectrum, we were able to calculate the ratio of CRABP:CRABP–ligand complexes at different concentrations of retinoic acid.

Figure 4a shows the data from the fluorimetric quenching experiments, in which the intensity of fluorescence emitted by CRABP or its mutants at 324 nm (the wavelength of maximum emission) is plotted against increasing concentrations of retinoic acid. As the concentration of retinoic acid is increased, the intensity of fluorescence emitted by the wild-type CRABP decreases until the ligand-binding site is saturated. Fluorescence quenching caused by nonspecific binding of retinoic acid to protein, assayed by using *N*-acetyl-L-tryptophanamide instead of a protein, is negligible in the concentration range used here. Compared to the wild-type CRABP, much less quenching of fluorescence was observed when CRBPII or mutants of CRABP were incubated in the presence of ligand. The intrinsic fluorescence of wild-type CRABP declined in an exponential fashion as a function of ligand concentration; while the fluorescence of CRBP II and mutant forms of CRABP were also quenched by increasing concentrations of retinoic acid, but apparently with much reduced affinities. Using Eqs. (1) and (2), $P_0\alpha$ was plotted against $R_0\alpha/(1-\alpha)$ (Fig. 4b). The affinity of wild-type CRABP for retinoic acid was determined to be $K_d = 39$ nM. Apparent dissociation constants (K_d) have been observed to range between 4 to 40 nM in previous studies.[3,32,33] The calculated number of apparent binding sites (n) was 1.0 (Materials and Methods).

Interactions of the proteins with retinoic acid

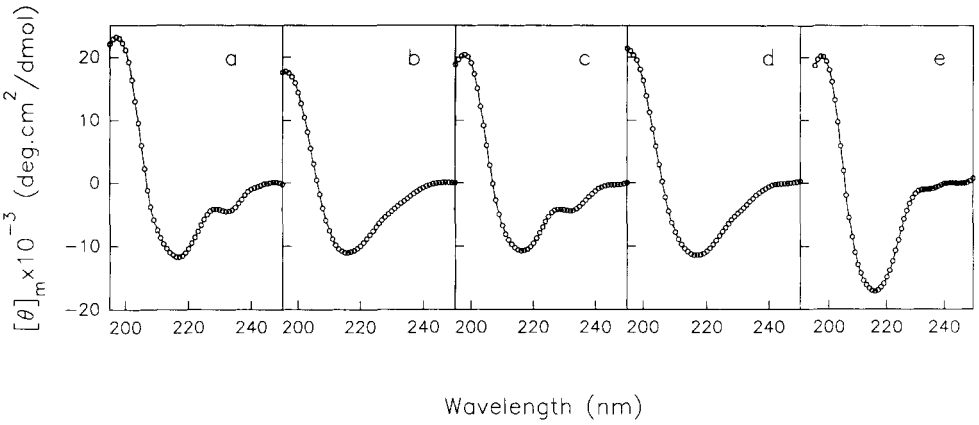

Fig. 3. Circular dichroism spectra of wild type and mutant versions of CRABP. Proteins were prepared in 2 mM Tris-Cl pH 8.3, the pathlength was 2 mm. Each spectrum represents the average of 3 scans, averaging time for each scan at each wavelength is 3 sec. (**a**) Wild-type CRABP; (**b**) single mutant R111Q; (**c**) single mutant R131Q; (**d**) double mutant R111Q,R131Q; (**e**) CRBPII.

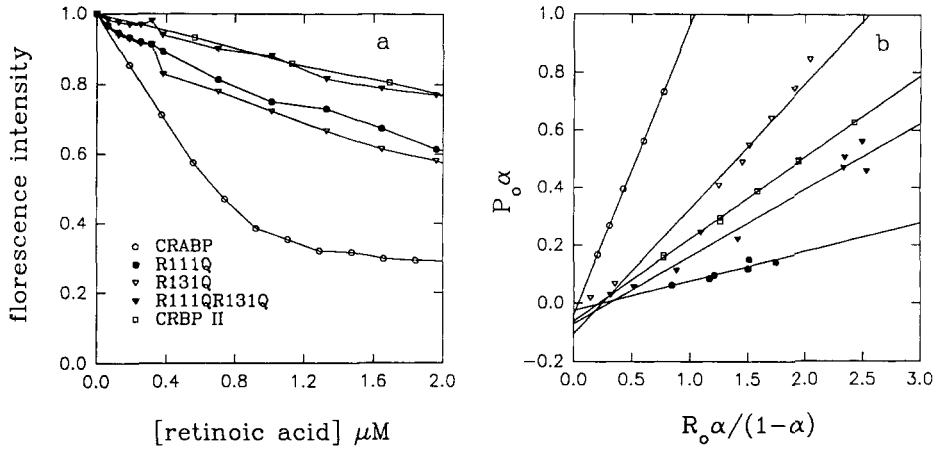

Fig. 4. (**a**) Fluoremetric titration assays for wild-type and mutant CRABP. The relative fluorescence intensity was plotted against concentration of added retinoic acid. (**b**) α (the fraction of free binding sites) was calculated by Eq. (2) and plotted against $R_0\alpha/(1-\alpha)$ (see Materials and Methods) for all the wild-type and mutant versions of CRABP. Wild-type CRABP (○); single mutant R111Q of CRABP (●); single mutant R131Q of CRABP (▽); double mutant R111QR131Q of CRABP (▼); CRBPII (□). The slope gives the number of binding sites (n) on the molecule, the intercept on Y axes gives the K_d/n.[22,23]

were further analyzed by circular dichroism (CD) in the near UV wavelength range (300 to 450 nm). Nonchiral retinoids are devoid of circular dichroism when they are free in solution. However, upon binding of retinoic acid to wild-type CRABP, the protein–retinoic acid complex shows induced CD in the region where retinoic acid absorbs. When both the proteins and the retinoic acid were used at a concentration of 20 μM, induced CD spectra were observed for the wild-type protein and for the R131Q mutant in the wavelength range between 320 and 360 nm (Fig. 5a, 5c). However, even when a 5-fold excess of retinoic acid (100 μM) was added to the solution, the R111Q mutant of CRABP (at 20 μM) did not show an induced CD (Fig. 5b). Results similar to those obtained for the R111Q mutant have been observed with the double mutant (R111Q,R131Q) in CD spectra with retinoic acid (data not shown). These observations support the binding mode between retinoic acid and CRABP proposed in Figure 1A, in which Arg-111 is directly involved in the interaction with retinoic acid while Arg-131 indirectly affects retinoic acid binding through Tyr-133. In the crystal structure of both P2 and I-FABP, Arg-106 (corresponding to the position of Arg-111 of CRABP) is directly involved in the ligand binding, while Arg-126 (corresponding to the position of Arg-131 of CRABP) is not.[12] CD experiments presented here suggest that analogous molecular mechanisms for the interactions between CRABP and retinoic acid may be present (see Discussion).

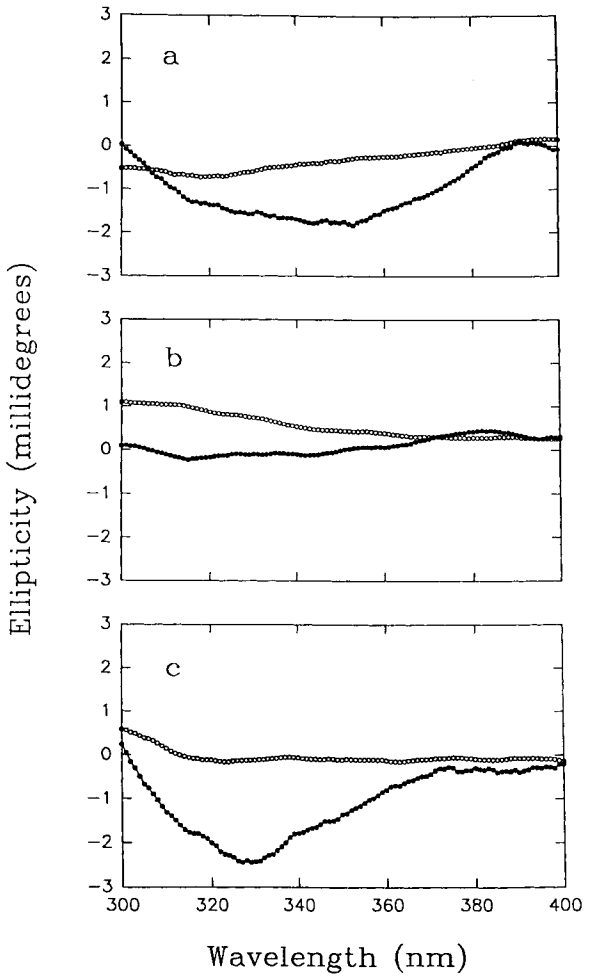

Fig. 5. Circular dichroism spectra of wild type and mutant CRABP with and without retinoic acid. All protein solution (concentration 20 μM) were prepared in 10 mM Tris-Cl pH 8.3. The pathlength was 5 mm. Each spectrum represents the average of 3 scans, averaging time for each scan at each wavelength is 3 sec. (**a**) 20 μM CRABP (○), 20 μM CRABP + 20 μM retinoic acid (●). (**b**) 20 μM R111Q (○), 20 μM R111Q + 80 μM retinoic acid (●). (**c**) 20 μM R131Q (○), 20 μM R131Q + 80 μM retinoic acid (●).

Thermostability of Wild-Type and Mutant Versions of CRABP

In I-FABP, myelin P2 protein and CRABP, the interiors of the β-barrel are filled mostly with the side chains of neutral and hydrophobic amino acid residues. Given the close packing of side chains, it is tempting to predict that if the charged side chains of bulky amino acids Arg-111 and Arg-131 are accommodated inside the pocket, they would energetically destabilize the protein in the absence of ligand.

The thermal unfolding of wild-type and mutant versions of CRABP shows cooperativity, as has been observed for many proteins. In Figure 6, the results are expressed as the fraction of unfolded protein observed at a series of temperatures. The melting temperature (T_m) is defined as the temperature when 50% of the protein is in an unfolded form. Thermal unfolding curves taken at a different wavelength do not deviate from the ones taken at wavelength 205 nm. Virtually identical thermodenaturation curves have been obtained with wild-type CRABP when CD measurements were taken at 216 nm. Figure 6 shows the following: (1) In the presence of retinoic acid, the melting temperature of wild-type CRABP is increased by 17°C. (2) In the absence of retinoic acid, the melting temperatures of the single mutants are 9.4°C (R111Q) and 11.6°C (R131Q) higher than that of wild-type CRABP. (3) In the presence of retinoic acid, none of the mutants of CRABP displays any changes (<1°C) in thermostability. (4) The CRBPII/retinol complex has 6.4°C higher melting temperature than the CRBPII apoprotein.

To estimate the contributions of ligand binding to the stabilization of CRABP and CRBPII in the holoproteins, and how much stabilization energy can be attributed to specific amino acids in the mutant versions of CRABP, the alterations of free energy changes in unfolding, $\Delta(\Delta G)$, were calculated from the denaturation curves. These alterations reflect the differences in thermostabilization energy between mutant versions of protein (or ligand-bound protein) and wild-type protein.[26,27] The results are summarized in Table III. It can be noted that the substitutions of either Arg-111 and Arg-131 by glutamines result in 3.0 and 3.7 kcal/mol increase in free energy of stabilization, respectively, which is comparable to the energy provided by hydrogen-bonded ion pairs.[34] The double mutant has a higher $\Delta(\Delta G)$ than either of the two single mutants, although it is not quite the sum of the two. The retinoic acid–CRABP complex has 5.6 kcal/mol increase in free energy of stabilization, which is probably a combined effect of ion-pair interactions between the arginine residues and the carboxyl group of the ligand, and other hydrophobic interactions between residues in the binding pocket and the retinoic acid. This point could be further substantiated by comparing the retinol-binding effect on CRBPII and the retinoic acid-binding effect on CRABP. From that comparison, the free energy change upon binding contributed by retinol to CRBPII is smaller than the change contributed by retinoic acid to CRABP.

DISCUSSION

Through a combination of homology-based structural modeling and site-specific mutagenesis of CRABP, we have explored the importance of interior arginine residues in ligand binding. As anticipated, both Arg-111 and Arg-131 play a role in binding to the negatively charged retinoic acid ligand. These residues correspond to residues implicated in ligand binding by other proteins in the same family as CRABP that also bind to carboxylates (adipocyte

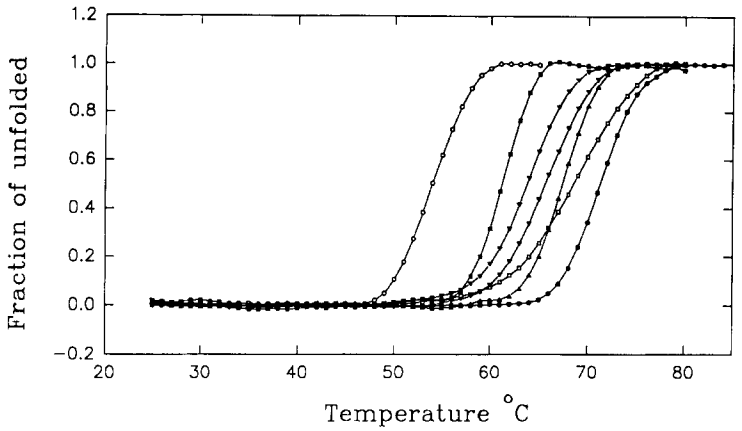

Fig. 6. Thermodenaturation curve of wild-type CRABP (○), wild-type CRABP + retinoic acid (●), single mutant R111Q (▽), single mutant R131Q (▼), double mutant R111QR131Q (□), CRBPII (■), and CRBPII + retinol (△). Temperature denaturation were monitored by their circular dichroism at 205 nm. The results are the averages from three experiments. Protein solutions were prepared in 10 mM potassium phosphate buffer. 2 mm pathlength cell was used. The heating rate 2 min/°C was used in all the experiments.

TABLE III. Analysis of Thermal Unfolding Curves for CRABP and Its Variants*

Protein	T_m(°C)	$\Delta(T_m)$ (°C)	$\Delta(\Delta G)$ (kcal/mol)
CRABP	54.0		
CRABP + RA	71.3	17.3	5.6
R111Q	63.6	9.4	3.0
R131Q	65.6	11.6	3.7
R111QR131Q	68.5	14.5	4.7
CRBPII	61.0		
CRBPII + R	67.4	6.4	2.1

*T_m is midpoint of thermal unfolding curve in °C. $\Delta(T_m)$ is the difference between the T_m values from the wild type. $\Delta(\Delta G) = [\Delta(T_m)] \times \Delta S_m = [\Delta(T_m)] \times (\Delta H_m/T_m)$, where ΔS_m and ΔH_m are values for the wild-type protein calculated from the slope and Y axis intersection of ΔG vs. T curve at the melting temperature.

and myelin P2 proteins and the various fatty acid binding proteins).

However, Arg-111 and Arg-131 interact in different ways with retinoic acid. From the modeled structure of the retinoic acid–CRABP complex, Arg-111 is predicted to bind directly to the carboxylate of the ligand while Arg-131 is predicted to hydrogen-bond to neighboring Tyr-133, which in turn interacts with the ligand. Mutants of CRABP display reduced binding of retinoic acid, but by monitoring induced CD in the ligand absorption region, we found that the R131Q mutant retains a weak but specific interaction with the ligand. This result lends credence to a binding mechanism analogous to that observed in the crystal structure of both P2 and I-FABP, where one arginine (106 in P2 and I-FABP) interacts directly with the ligand and the other does not (in proximity in the P2 case and interacting with Asp-34 in I-FABP).

Consistent with our conclusions about the importance of Arg-111 for ligand binding in CRABP are results of a recent study in which mutations were introduced into CRBP to change its binding specificity.[35] By mutating the residue (Gln-108) that corresponds to Arg-111 in CRABP to an arginine, the authors created a mutant CRBP that had significantly higher affinity for carboxylate-containing ligands. We do not find the converse to be true, i.e., our mutants of CRABP do not display higher binding to retinol or retinal than the wild-type CRABP. The different effects from alteration of binding residues may reflect the enhanced specificity of CRABP for its ligand. Wild-type CRBP is far less discriminating between ligands than CRABP, and the mutation made it even less so. By contrast, CRABP strongly prefers retinoic acid, and the mutants show a reduced affinity for the ligand, retinoic acid, without creating experimentally detectable enhancements in binding of neutral retinoids. In a further study to understand the interaction between CRABP and retinoic acid, and to see if we could create a higher retinol binding affinity by mutagenizing CRABP, we also replaced Tyr-133 with Phe in the double mutant R111Q,R131Q. From sequence alignment of this family of proteins[10] and the CRABP model structure, Tyr-133 is implicated in the hydrogen bond network, conserved among the family of proteins whose ligands contain carboxylates, but replaced by phenylalanine in CRBP and CRBPII whose ligands contain neutral groups. Replacing Tyr-133 with Phe did not alter the predominant β structure, as was indicated by comparing the measured CD spectra of the triple mutant CRABP with other CRABP mutants. Meanwhile, this additional mutation did not increase the binding affinity of mutant CRABP to retinol, nor to retinal (data not

shown). Our explanation is that the interactions between the hydrophobic parts of the retinol or retinal and CRBP or CRBP II are more important than these interactions between retinoic acid and CRABP. The interaction between the carboxylate of retinoic acid and CRABP is strong enough to stabilize the binding. Therefore, substituting the interior glutamine by arginine (position 106 in CRBP is aligned to arginine 111 in CRABP) may have created a strong interaction between the carboxylate of retinoic acid and the mutated CRBP. On the other hand, creating the specific interactions between the engineered CRABP and retinol may require replacement of many residues to accumulate a significant effect in retinol binding from multiple weaker interactions between the protein and the ligands. Once again, we wish to emphasize that the atomic level detail in the interpretation of retinoic acid binding results relies on the accuracy of our model structure which is based on the crystal structure of a homologous protein. Solving the three-dimensional structures of CRABP and its mutants should shed light on the specific interaction that account for ligand-binding specificities in this group of proteins.

The mutations we introduced (that change Arg-111 and Arg-131 to glutamines) appear to be tolerated in large part without disruption of the native CRABP structure. However, differences are observable between the mutants and the wild-type CRABP CD spectra. Wild-type CRABP shows a well-defined shoulder on the long wavelength side (around 230 nm) of the major minimum (which occurs at 216 nm). This feature is present in the R131Q mutant, but is absent in the R111Q and R111Q,R131Q mutants. The 230 nm CD bands seen in wild-type and R131Q mutant CRABP are not likely of α helical origin, since the diagnostic CD bands for α structure are at 208 and 222 nm.[28–31] On the other hand, it is known that the absorption wavelength for the aromatic residues is around 230 nm, and CD bands around 230 nm indeed have been observed to be generated by aromatic residues.[36] Moreover, it has also been suggested that positively charged side chains make enthalpically favorable intersections with the π electron clouds of aromatic side chains.[37,38] Therefore, it is likely that the interactions between the aromatic residue (Trp-109) in the binding pocket and Arg-111 affect the local environments and packing that could bring about the modifications in CD spectra in mutants R111Q and R111Q,R131Q. Thus, substitution of Arg-111 by Gln, a mutation which gave the more pronounced effect on ligand binding, also gives the most detectable perturbations on the side chain packing near the binding pocket. Further experiments are in progress to separate the effects of tertiary structural alterations from the contributions of individual side chains to binding.

The need for a cavity capable of binding a ligand that is at once hydrophobic and negatively charged appears to have compromised the stability of ligand-free CRABP. This lower stability of apoprotein compared to the holoprotein may serve the purpose of enabling the protein to open up more readily and provide access of the ligand to its binding site. The stabilities of CRABP in its ligand-free and ligand-bound forms and of the mutants with arginine substitutions follow an order that is consistent with a pronounced destabilizing electrostatic effect from buried positive charge. Compensation of one charge by ligand stabilized the protein by ~6 kcal/mol, whereas removal of the charge by mutagenesis stabilized CRABP by ~3 kcal/mol. The difference between the stabilization from ligand binding and that from removal of a charge most likely reflects the hydrophobic interactions of the retinoid.

The Arg residues in the interior of CRABP may provide not only electrostatic interactions that stabilize ligand once bound to the protein, but also a positive electrostatic potential field that guides the entrance of retinoic acid into the binding pocket. The calculated electrostatic potential of CRABP (see Results) reveals a positive potential extends to the inside of the β-barrel. This path is provided by Arg-111 and Arg-131. Analogous electrostatic influences on ligand binding have been postulated for other proteins, notably superoxide dismutase, and are believed to facilitate greatly the interaction of free ligand with protein.[39,40]

ACKNOWLEDGMENTS

We wish to thank Gail Martin for mouse embryo gt10 library, Jeff I. Gordon for the CRBPII cDNA clone, and Sherry Mowbray and Larry Dick for guidance with protein purification. This work was supported by grants to J.F.S. and L.M.G. from the National Institutes of Health. L.M.G. thanks the Robert A. Welch Foundation for continued support. T.A.J. is supported by the Swedish National Science Research Council.

REFERENCES

1. Sweetser, D.A., Heukeroth, R.O., Gordon, J.I. The metabolic significance of mammalian fatty-acid-binding proteins: abundant proteins in search of a function. Annu. Rev. Nutr. 7:337–359, 1987.
2. Chytil, F., Ong, D.E. Intracellular vitamin A-binding proteins. Annu. Rev. Nutr. 7:321–335, 1987.
3. Chytil, F., Ong, D.E. Cellular retinoid-binding proteins. In: "The Retinoids." Sporn, M.B., Robert, A.B., Goodman, D.S. (eds.). Orlando, FL: Academic Press, 1984:90–125.
4. Roberts, A.B., Sporn, M. Cellular biology and biochemistry of the retinoids. In: "The Retinoids." Sporn, M.B., Robert, A.B., Goodman, D.S. (eds.). Orlando, FL: Academic Press, 1984:210–287.
5. Dolle, P., Ruberte, E., Leroy, P., Morriss-Kay, G., Chambon, P. Retinoic acid receptors and cellular retinoid binding proteins. I. a systematic study of their differential pattern of transcription during mouse organogenesis. Development 110:1133–1151, 1990.
6. Petkovich, M., Brand, N.J., Krust, A., Chambon, P. A human retinoic acid receptor which belongs to the family of nuclear receptors. Nature (London) 330:444–450, 1987.
7. Giguere, V., Ong, E.S., Segue, P., Evans, R.M. Identifica-

tion of a receptor for the morphogen retinoic acid. Nature (London) 330:624–629, 1987.
8. Barkai, U., Sherman, M.I. Analysis of the interactions between retinoid-binding proteins and embryonal carcinoma cells. J. Cell. Biol. 104:671–678, 1987.
9. Maden, M., Ong, E.E., Summerbell, D., Chytil, F. Spatial distribution of cellular protein binding to retinoic acid in the chick limb bud. Nature (London) 335:733–735, 1988.
10. Jones, T.A., Bergfors, T., Sedzik, J., Unge, T. The three-dimensional structure of P2 myelin protein. EMBO J. 7: 1597–1604, 1988.
11. Sacchettini, J.C., Gordon, J.I., Banaszak, L.J. Refined apoprotein structure of rat intestinal fatty acid binding protein produced in E. coli. Proc. Natl. Acad. Sci. USA 86: 7736–7740, 1989.
12. Sacchettini, J.C., Gordon, J.I., Banaszak, L.J. Crystal structure of rat intestinal fatty-acid binding protein. Refinement and analysis of the E. coli-derived protein with bound palmitate. J. Mol. Biol. 208:327–339, 1989.
13. Shubeita, H.E., Sambrook, J.F., McCormick, A.M. Molecular cloning and analysis of functional cDNA and genomic clones encoding bovine cellular retinoic acid-binding protein. Proc. Natl. Acad. Sci. U.S.A. 84:5645–5649, 1987.
14. Zhang, J. Structure/function studies of cellular retinoic acid binding protein (CRABP). Ph.D. thesis, University of Texas Southwestern Medical Center, 1991.
15. Sambrook, J.F., Fritsch, E.F., Maniatis, T. "Molecular Cloning: A Laboratory Manual." Cold Spring Harbor, NY: Cold Spring Harbor Laboratory, 1989.
16. DISCOVER, HOMOLOGY, AND DELPHI are commercially available from Biosym Technologies, 10065 Barnes Canyon Road, San Diego, CA 92121.
17. Jones, T.A., and Thirup, S. Using known substructures in protein model building and crystallography. The EMBO J. 5:819–822, 1986.
18. Stam, C.H. The crystal structure of a monoclinic modification and the refinement of a triclinic modification of vitamin A acid (retinoic acid), $C_{20}H_{28}O_2$. Acta Crystallogr. B28:2936, 1972.
19. Dauber-Osguthorpe, P., Roberts, V.A., Osguthorpe, D.J., Wolf, J., Genest, M., Hagler, A.T. Structure and energetics of ligand binding to proteins: *Escherichia coli* dihydrofolate reductase-trimethoprim, a drug-receptor system. Proteins 4:31–37, 1988.
20. Gilson, M., Sharp, K., Honig, B. Calculated the electrostatic potential for molecules in solution. J. Comp. Chem. 9:327–335, 1987.
21. Gilson, M., Honig, B. Calculations of electrostatic potentials in an enzyme active site. Nature (London) 330:84–86, 1987.
22. Zoller, M.J., Smith, M. Oligonucleotide-directed mutagenesis: A simple method using two oligonucleotide primers and a single-stranded DNA template. Methods Enzymol. 154:329, 1987.
23. Tabor, S., Richardson, C.C. A bacteriophage T7 RNA polymerase/promoter system for controlled exclusive expression of specific genes. Proc. Natl. Acad. Sci. U.S.A. 82: 1074–1078, 1985.
24. Li, E., Locke, B., Yang, N.C., Ong, D.E., Gordon, J.I. Characterization of rat cellular retinol-binding protein II expressed in Escherichia coli. J. Biol. Chem. 262:13773–13779, 1987.
25. Cogan, U., Kopelman, M., Mokady, S., Shinitzky, M. Binding affinities of retinol and related compounds to retinol binding proteins. Eur. J. Biochem. 65:71–78, 1976.
26. Pace, C.N., Shirley, B.A., Thomson, J.A. Measuring the conformational stability of a protein. In: "Protein Structure, a Practical Approach." Creighton, T.E. (ed.). IRL Press: Oxford, U.K. 1988:311–330.
27. Becktel, W.J., Schellman, J.A. Protein stability curves. Biopolymers 26:1859–1877, 1987.
28. Johnson, W.C., Jr. Secondary structure of proteins through circular dichroism spectroscopy. Annu. Rev. Biphys. Chem. 17:145–166, 1988.
29. Woody, R.W. Circular dichroism of peptides. Peptide 7:15–114, 1985.
30. Yang, J.T., Wu, C.-S.C. Calculation of protein conformation from circular dichroism. Methods Enzymol. 130:208–269, 1986.
31. Johnson, W.C. Protein secondary structure and circular dichroism: A practical guide. Proteins 7:205–214, 1990.
32. Jetten, A.M., Jetten, M.E.R. Possible role of retinoic acid binding protein in retinoic stimulation of embryonal carcinoma cell differentiation. Nature (London) 278:180–182, 1979.
33. Siegenthaler, G., Saurat, J.-H. A slab gel electrophoresis technique for measurement of plasma retinol-binding protein, cellular retinol-binding and retinoic-acid-binding proteins in human skin. Eur. J. Biochem. 166:209–214, 1987.
34. Fersht, A.R., Shi, J.-P., Knill-Jones, J., Lowe, D.M., Wilkinson, A.J., Blow, D.M., Brick, P., Carter, P., Waye, M.M.Y., Winter, G. Hydrogen bonding and biological specificity analyzed by protein engineering. Nature (London) 314:235–238, 1985.
35. Stump, D.G., Lloyd, R.S., Chytil, F. Site-directed mutagenesis of rat cellular retinol-binding protein. J. Bio. Chem. 266:4622–4630, 1991.
36. Day, L.A. Circular dichroism and ultraviolet absorption of a deoxyribonucleic acid binding protein of filamentous bacteriophage. Biochemistry 12:5329–5339, 1973.
37. Burley, S.K., Petsko, G.A. Aromatic-aromatic interaction: A mechanism of protein structure stabilization. Science 229:23–28, 1985.
38. Burley, S.K., Petsko, G.A. Amino-aromatic interactions in proteins. FEBS Lett. 203:125–189, 1986.
39. Klapper, I., Hagstrom, R., Fine, R., Sharp, K., Honig, B. Focusing of electric fields in the active site of Cu-Zn superoxide dismutase: Effect of ionic strength and amino-acid modification. Proteins 1:47–59, 1986.
40. Getzoff, E.D., Tainer, J.A., Weiner, P.K., Kollman, P.A., Richardon, J.S., Richardon, D.S. Electrostatic recognition between superoxide and copper, zinc superoxide dismutase. Nature (London) 306:287–290, 1983.